JOC The Journal of Organic Chemistry

Article

pubs.acs.org/joc

Rotational Energy Barrier of 2-(2′,6′-Dihydroxyphenyl)benzoxazole: A Case Study by NMR

Weihua Chen, Eric B. Twum, Linlin Li, Brian D. Wright, Peter L. Rinaldi, and Yi Pang*

Department of Chemistry & Maurice Morton Institute of Polymer Science, The University of Akron, Akron, Ohio 44325, United States

Supporting Information

ABSTRACT: 2-(2′-Hydroxyphenyl)benzoxazole (HBO) derivatives represent an important class of luminescent materials, as they can undergo excited state intramolecular proton transfer (ESIPT). The material's ESIPT properties are dependent on the ratio of two different rotamers, whose interconversion is poorly understood. By using HBO derivative **4**, the rotational energy barrier of 2- (2′,6′-hydroxyphenyl)benzoxazole is determined to be 10.5 kcal/mol by variable-temperature NMR. Although a HBO derivative typically exhibits two rotamers with O···H−O (e.g., **1a**) and N···H−O bonding (e.g., **1b**), correlation of NMR with fluorescence data reveals that the rotamer with N···H−O bonding is predominant in the solution.

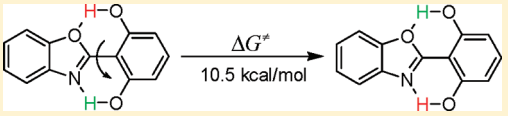

INTRODUCTION

2-(2′-Hydroxyphenyl)benzoxazole (HBO, **1**) has emerged to be an interesting luminescent material that exhibits large Stokes' shift arising from the excited-state intramolecular proton transfer (ESIPT).[1] The unique optical characteristics have resulted in various applications including chemical sensors for zinc(II)[2−5] and anions,[6] light-emitting diode devices,[7] and optical switching.[8] Although the HBO molecule can exist in the intramolecular hydrogen-bonded rotamers **1a** and **1b** (Scheme 1), only the latter is thought to undergo ESIPT.[9,10] X-ray diffraction reveals that the two rotamers **1a** and **1b** exist in about a 1:1 ratio in the crystalline state,[11] with the hydroxyl group pointing to either the N- or O-atom side of the oxazole ring. Significant interest exists in elucidating the ESIPT process (Scheme 2) and to discover the underlying principles that govern the rotamer ratio **1a** and **1b** and their conversion. Fluorescence of a HBO typically gives both *enol* and *keto* emission. Practically, it is desirable to control the HBO in rotamer **1b** for optimized *keto* emission, as ESIPT is currently emerging as one of the appealing new mechanisms for chemosensors.[12] Unfortunately, our knowledge about the relative population of these rotamers in the sample is very limited, except a few scattered cases of studies being reported from crystal structures of HBO derivatives.[11,6] Although a fluorescence study shows that the relative population of **1b** in solution increases at low temperature,[13] few attempts have been

Scheme 1. Structures of HBO Derivatives[a]

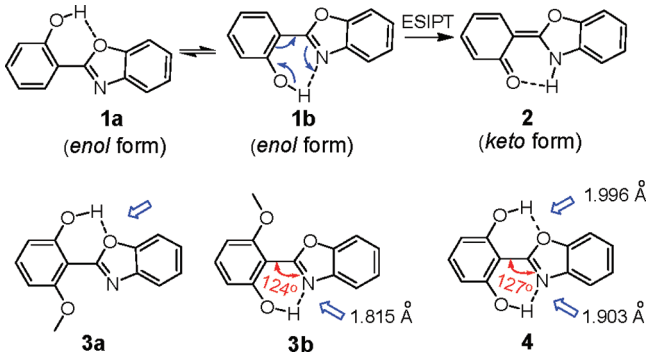

[a]The thick arrows indicate the H-bond locations in **3** and **4**. The hydrogen bond lengths and bond angles of **3b** and **4** are from their corresponding crystal structures.

Scheme 2. Schematic Illustration for ESIPT of HBO Derivatives

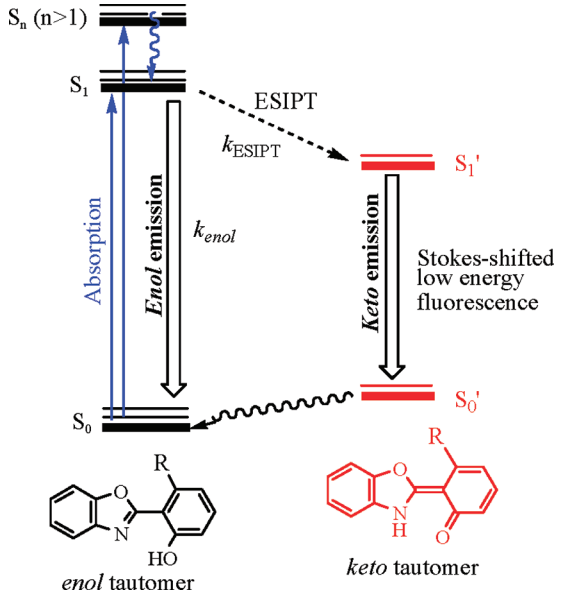

Received: September 13, 2011
Published: November 21, 2011

   dx.doi.org/10.1021/jo201890f | J. Org. Chem. 2012, 77, 285−290

made to characterize the rotamer population in solution. Lack of a spectroscopic method to identify the specific rotamer(s), in addition to the absence of a suitable model system, makes the problem a challenging issue.

Conversion between **1a** and **1b** occurs via rotating the bond between 2-hydroxyphenyl and oxazole units. Quantum calculations have predicted the interconversion barrier to be ~2.5 kcal/mol (by CDDO/S-CI)[13] or ~15 kcal/mol (by ab initio with the STO-3G basis set).[14] The lack of convenient methods to distinguish between the two different hydrogen-bonding modes (i.e., O···H−O and N···H−O), in addition to their reversible nature, makes it difficult to experimentally evaluate the rotation barrier in solution. Extending our general interest in exploring the fluorescence of ESIPT,[4,6,15,16] we now report the rotational barrier of 2-(2′,6′-dihydroxyphenyl)benzoxazole **4**, which is determined by variable-temperature NMR. In conjunction with crystal structure and fluorescence spectroscopy, ^{1}H NMR of HBO compounds **1** and **3** also reveals that the rotamer ratio found in the crystalline sample could be very different from that in solution. This study thus sheds some light on the identity of HBO rotamer in solution, as most ESIPT-based dyes are expected to be used in the solvent.

RESULTS AND DISCUSSION

The HBO derivatives **3** and **4** were synthesized as reported previously.[15] Interestingly, the crystal structure of **3** revealed *only* one rotamer with the hydroxyl group pointing to the N-atom in the solid (Figure 1). The result is in sharp contrast

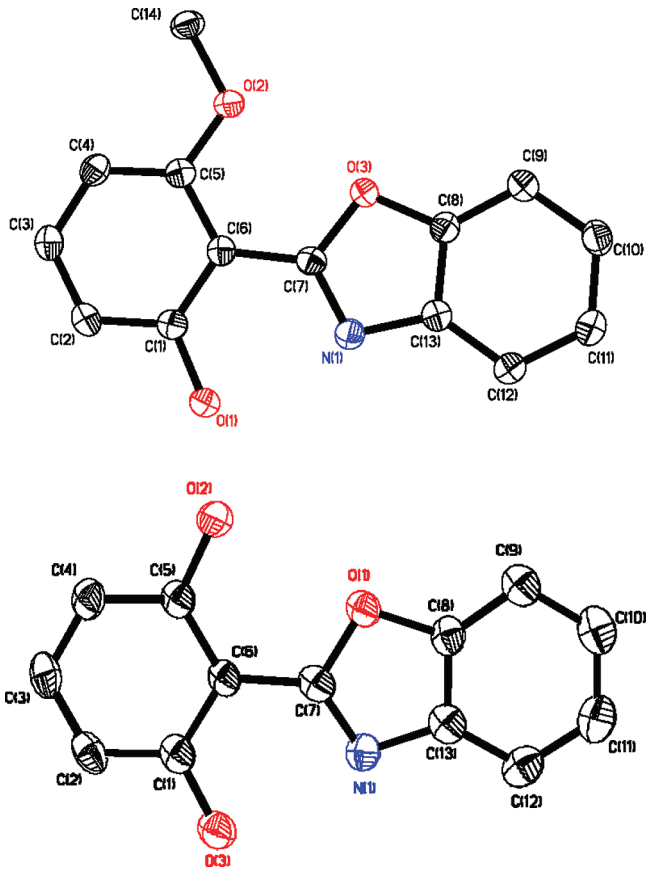

Figure 1. ORTEP plot of the crystals **3** (top) and **4** (bottom).

to crystalline **1**, where two rotamers are found in 1:1 ratio.[11] The results indicated that the crystal packing could play a significant role in determining the rotamer ratio of HBO. The crystal structure of **4** showed a planar geometry with concomitant N···H−O and O···H−O bonding. Analysis of hydrogen bond length showed that the N···H distance in the N···H−O bonding of **3** (1.815 Å) was shorter than that of **4** (1.903 Å), as the competitive O···H−O bond weakened the N···H−O bond in **4**.

Fluorescence of HBO **1** in solution is known to give *enol* and *keto* emission, which are related to the relative population of **1a** and **1b**. Only rotamer **1b** can undergo ESIPT and contribute to *keto* emission. In contrast, rotamer **1a** and some "solvated **1b**" are thought to give *enol* emission. The fluorescence of **4** revealed only *keto* emission in methylene chloride (Figure 2). In methanol, negligible *enol* emission became visible from **4**, possibly due to the formation of "solvated HBO". It was assumed that the *enol* emission from **1** and **3** were mainly attributed to the rotamers **1a** and **3a**, respectively. Although the crystalline **3** was found to have no rotamer **3a**, its *enol* emission in solution was relatively higher in intensity than **1**. Assuming that the radiative decay of the *enol* and *keto* tautomers are similar, the relative *enol* content of a HBO molecule could be represented approximately by its *enol* emission intensity. The higher *enol* emission thus indicated that the content of rotamer **3a** in the solution of **3** was higher than that of **1a** in the solution of **1**. The result also suggests that the rotamer ratio found in the solid state could be very different from the ratio present in solution.

Rotational Energy Barrier by Variable-Temperature ^{1}H NMR. Unlike **3**, rotation of the hydroxyphenyl fragment in **4** gives the same structure. This feature warrants that the proton in the O−H···N bond has an equal population as the proton in the O−H···O bond. It was assumed that the protons in the O−H···N and O−H···O bonding structures have considerably different chemical shifts, as ^{1}H NMR is sensitive to the hydrogen bonding environment.[17] Equal proton populations in O−H···N and O−H···O environments, in addition to a large difference in chemical shift, simplified the task of studying the rate of rotation by low-temperature NMR.[18]

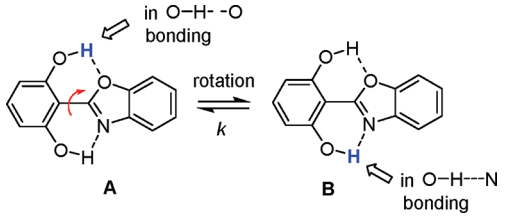

The ^{1}H NMR spectrum of **4** in $CDCl_3$ at 30 °C gave one broad peak at ~9.8 ppm (Figure 3a), which was attributed to the phenolic protons. Apparently, at temperatures higher than the coalescence temperature, "fast rotation" occurred and an average signal was observed for the two protons in the different H-bonding environments. As the temperature was decreased, the peak became broad. Two peaks emerged when the temperature was below −40 °C. In this case, at temperatures below the coalescence point, the bond rotation became slow compared to the NMR time scale. The resonance signals at ~12.2 and 7.9 ppm were assigned to O−H···N and O−H···O protons, respectively.

Spectral simulations (Figure 3b) were performed using WINNMR-pro,[19] which matched well with the experimental data. Determination of the coalescence temperature (T_c = −20 °C = 253K), in addition to the difference in chemical shift of the two

dx.doi.org/10.1021/jo201890f | J. Org. Chem. 2012, 77, 285−290

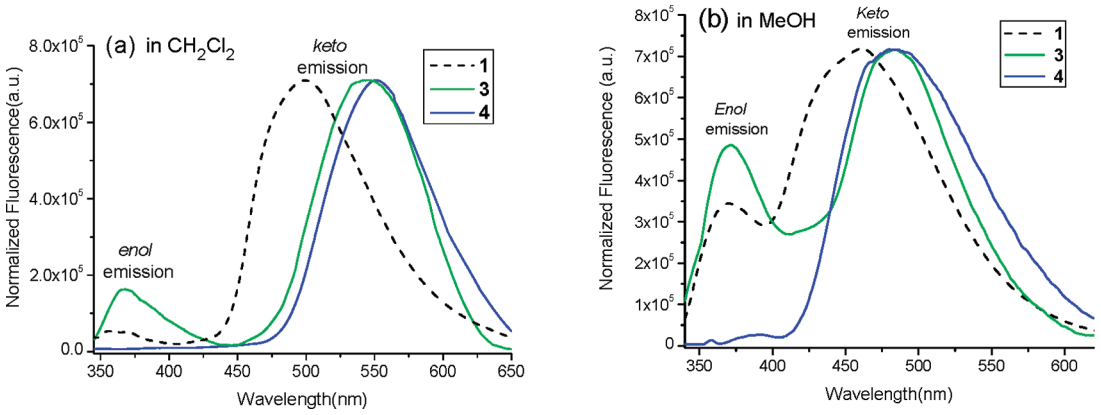

Figure 2. Normalized emission of **1** (HBO), **3** (MHBO), and **4** (DHBO) in CH_2Cl_2 (a) and methanol (b).

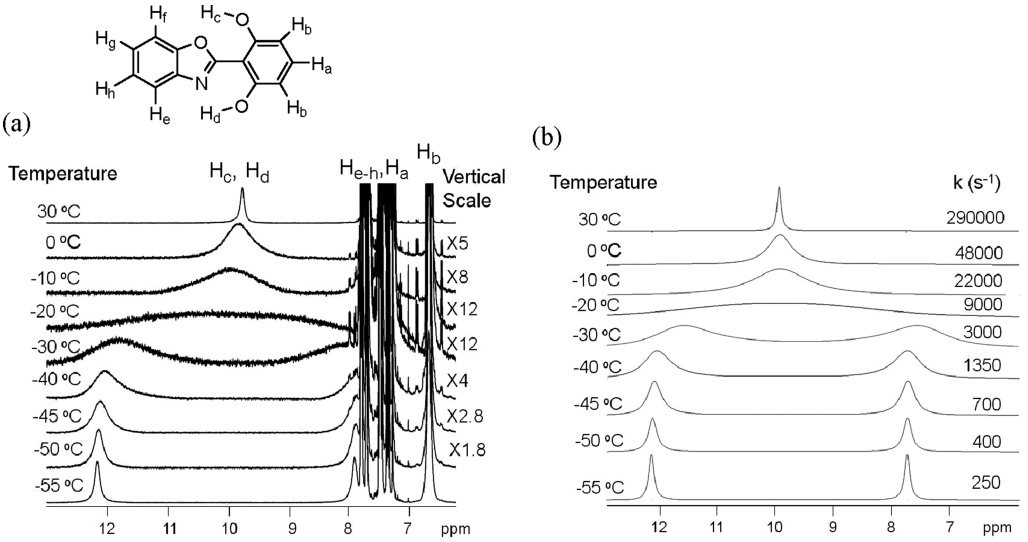

Figure 3. (a) 400 MHz variable-temperature ^{1}H NMR spectra of **4** (concertration: 25 mM in $CDCl_3$). The hydrogen-bonded protons were observed by starting from the fast exchange at 30 °C, passing through the coalescence temperature near −20 °C, and ending in the slow exchange at −40 °C or below. The signal at 7.25 ppm was attributed to residual $CHCl_3$ in the deuterated solvent. (b) Spectral simulations from dynamic NMR.

H-bonded protons, allowed calculation of the Gibbs free activation energy from the Eyring equation:

$$\Delta G^{\ddagger} = 2.303RT(10.319 + \log T_c - \log k_c)$$

$$=0.0191 \times T_c(9.97 + \log T_c - \log (\nu_A - \nu_B))$$

$$=0.0191 \times 253[9.97 + \log(253) - \log[400 \times (12.2 - 7.9)]]$$

$$=44.25 \text{ kJ/mol} = 10.59 \text{ kcal/mol}$$

where ν_A and ν_B are chemical shifts in Hz, R is the gas constant, T_c is the coalescence temperature (in K), and k_c is the rate constant at the coalescence temperature for interchange of rotamers **A** and **B**. The rotational barrier was assumed to be associated with breaking the intramolecular hydrogen bonds which hold two aromatic fragments in coplanarity. Observation of the same line broadening pattern at lower concentration (3.1 mM in $CDCl_3$) at variable temperature (Figure S6, Supporting Information) further confirmed that the intermolecular hydrogen bonding was not a significant factor in determining the rotation barrier. When the spectral data at coalescence was compared with the simulated spectra (Figure S9, Supporting Information), it was estimated that k_c could be determined with a relative error of ±10%.

Chemical Shift of O−H—N and O−H—O. Two phenolic protons of **4** at different chemical shifts (at 7.9 and 12.2 ppm) were attributed to different hydrogen-bonding environments, i.e., O···H−O and N···H−O bonding, respectively. Compound **3** can be used as a model compound to aid the assignments. As shown in Figure 1, only rotamer **3b** with N···H−O bonding was observed in the crystal structure of **3**. The ^{1}H NMR spectrum of **3** in $CDCl_3$ revealed a sharp peak at 12.7 ppm (Figure S1, Supporting Information), attributed to the proton in the N···H−O bonding rotamer. Therefore, the resonances of **4** at 12.2 and 7.9 ppm could be attributed to the N···H−O and O···H−O protons, respectively. The assignment was consistent with the chemical shift reported in benzofuran **5**, which can be regarded as a close model compound for the proton in the O···H−O bonding rotamer.[20]

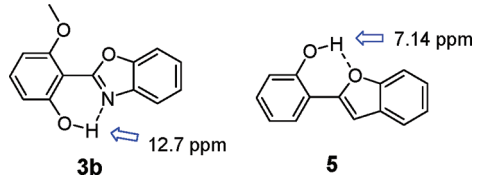

dx.doi.org/10.1021/jo201890f | J. Org. Chem. 2012, 77, 285−290

Scheme 3. *Enol* Rotamers of HBO in the Ground State

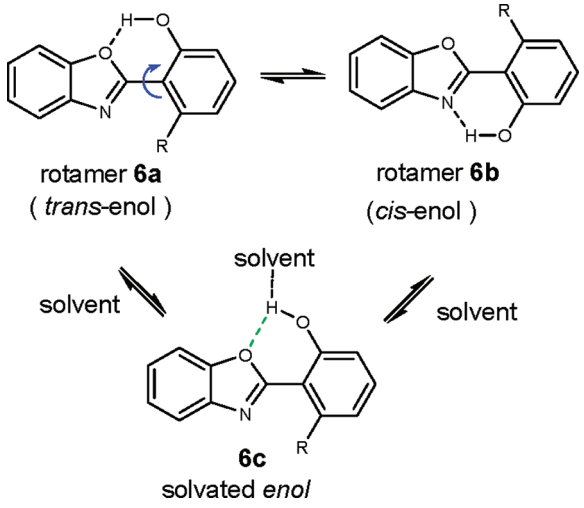

Spectroscopic Identification of Rotamer and *Enol* and *Keto* Emission. As shown in Scheme 2, the HBO molecule is driven to the excited state upon absorption of photons. The excited molecule can then return to its ground state to give *enol* emission, or undergo ESIPT to give *keto* emission. The *enol* can exist in different rotamers **6a** and **6b** (Scheme 3). It is generally agreed that only rotamer **6b** can undergo the ESIPT process to give the *keto* emission. In the excited state of DHBO **4**, the deactivation pathways are present for both *enol* emission and ESIPT, making the molecule a suitable probe to examine the competitive process between *enol* and *keto* emission. Exclusive *keto* emission was observed from DHBO **4** in CH_2Cl_2 (Figure 2a), hexanes, and CH_3CN,[15] showing that the ESIPT of **6b** was a more competitive process than the *radiative* deactivation of both *enols* **6a** and **6b**. In a protic solvent such as methanol, very weak emission was observed from the methanol solution of **4** (Figure 2b), suggesting the presence of solvated *enol* species **6c** (in addition to regular *enol* **6a** and **6b**). Predominant *keto* emission from **4**, however, indicated that the ESIPT process of **6b** is a much more competitive process, as ESIPT is a fast process, with the rate constant of ~150 fs being reported for HBO.[21]

Correlation between HBO structures and their *enol*/*keto* emission requires development of a strategy to identify the specific rotamers present in solution. The compound **3** serves as a suitable model, which is structurally similar to **4** but with only one hydroxy group to give two rotamers. The *phenolic* proton signal at 12.7 ppm in ^{1}H NMR indicated that **3** was present mainly in the form of rotamer **3b**. Negligible *enol* emission from **3** in CH_2Cl_2 (Figure 2a) was consistent with the assumption that rotamer **3b** was major. Although the *keto* emission remained to be predominant in methanol (a protic solvent), **3** gave noticeable *enol* emission (Figure 2). Since the *enol* emission from **6b** (= **3b** if R = $-OCH_3$) was less competitive (as seen from **4**), the observed increase in *enol* emission could be mainly attributed to the solvated *enol* **6c**.

A similar trend has been observed in the emission of **1**, which reveals the predominant *keto* emission in a nonpolar solvent such as hexane and CH_2Cl_2 (Figure 2a), but gives noticeable *enol* emission in a protic solvent such as methanol.[15] The ^{1}H NMR of **1** in $CDCl_3$ revealed the *phenolic* proton signal at ~11.45 ppm (Figure 4), whose intensity and peak width was not affected by varying the temperature between +50 and −50 °C (Figure S7, Supporting Information). The peaks of

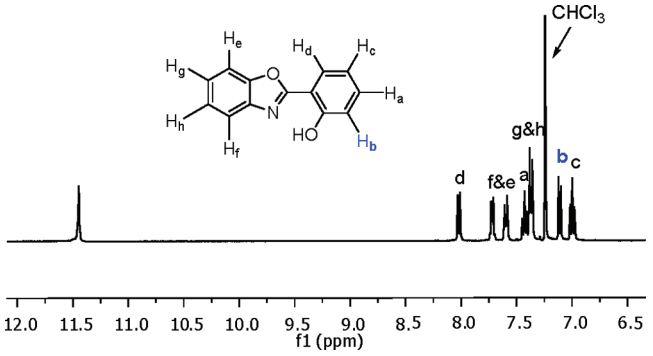

Figure 4. 400 MHz ^{1}H NMR of **1** (concentration: 3.1 mM in $CDCl_3$) at 30 °C.

phenolic and H_b protons of **1** were as narrow as the solvent peak, in sharp contrast to the significant peak broadening observed from the ^{1}H NMR spectrum of **4**. Lack of enol emission in the nonpolar solvent (e.g., CH_2Cl_2),[15] in addition to the chemical shift position, further supports the assignment of the signal at ~11.45 ppm to **1b** in chloroform. The results showed that the tautomer ratio of **1a**:**1b** (≈ 1:1) determined in the crystal of **1**[11] does not represent the ratio present in the solution (predominantly **1b**).

To further confirm the assignment for the rotamer **1b**, the model compound **7** (2-bromo-6-(4-methylbenzo[*d*]oxazol-2-yl)-phenol) was prepared by using the procedure reported previously.[22] The phenolic proton of **7** (Figure 5) gave a narrow resonance at ~11.5 ppm, in sharp contrast to that of **4** which produced a

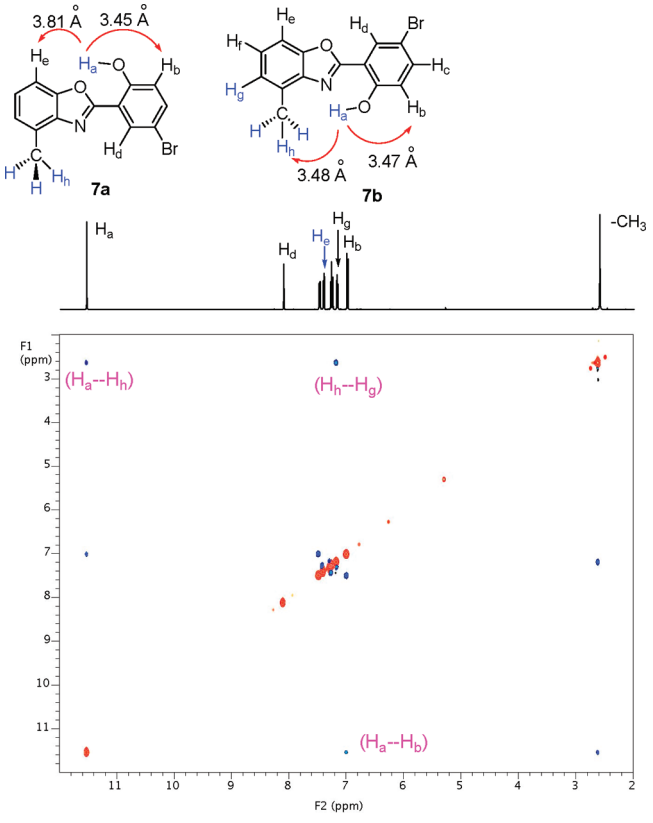

Figure 5. (Top) Structure of rotamers **7a** and **7b**, with proton−proton distances marked on the arrows. (Bottom) 400 MHz ^{1}H NOESYspectrum of 7′-MeHBO **7** in $CDCl_3$ shows correlation between phenolic proton H_a and aromatic proton H_b.

dx.doi.org/10.1021/jo201890f | J. Org. Chem. 2012, 77, 285−290

broad −OH resonance (Figure 3). The 2D NOESY spectrum showed that the −OH group (H_a at 11.55 ppm) had NOESY correlations with the methyl group resonance (H_h at 2.63 ppm) and the adjacent aromatic proton resonance (H_b at 7.02 ppm). The observed NOESY correlation between −OH and methyl protons confirmed the presence of the *cis*-enol form **7b** in solution. In rotamer **7a**, the proton−proton distance between the −OH (H_a) and methyl (H_h) hydrogens are calculated to be 6.6 Å, which is too large to produce NOESY correlations.[23] It should be noted that the phenolic protons H_a in **7a** and **7b** exhibit NOE effects on different protons. In the rotamer **7b**, the H_a has an NOE effect on the methyl proton H_h and aromatic proton H_b. This is in sharp contrast to H_a in the rotamer **7a**, which has an NOE effect on two aromatic protons H_b and H_e. Absence of a cross peak between the resonances of H_a and H_e suggests that the rotamer **7a** was either not present in the solution or at a concentration below the detection limit. The assumption (i.e., the absence of **7a**) is in agreement with the sharp signal of H_d, which is expected to have different chemical shifts in the rotamers **7a** and **7b**. Therefore, the compound exists mainly as the rotamer **7b** in the solution. Since the phenolic protons in both **1** and **7** have very similar chemical shift ($\delta \approx 11.5$ ppm), we can conclude that the rotamer **1b** is the predominant form in solution.

It should be pointed out that the rotational energy barrier was determined from **4**, where a second −OH was introduced to facilitate the detection of both N···H−O and O···H−O hydrogen-bonded protons. The presence of the second hydrogen bonding, i.e., O···H−O in **4**, could further restrict the rotation of benzoxazole. Therefore, the rotational energy barrier from **4** (∼10.59 kcal/mol) could be higher than that from mono(HBO) **1**. The results clearly indicated that the previous estimation of the rotational barrier for **1** (∼15 kcal/mol by ab initio with STO-3G basis set) was incorrect.[14] Deviation of the rotational barrier from **1** is dependent on the impact of the additional hydrogen bonding O···H−O in **4**. The crystal structure of **4** showed that the N···H distance in the N···H−O bond was 1.903 Å, which was shorter than the O···H distance (1.996 Å) in O···H−O bond. The rotational barrier of **4** could be largely determined by the stronger N···H−O bond, as the hydrogen bond O···H−O is relatively weak. It should also be noted that the impact of the O···H−O bond on the rotational barrier of **4** was partially offset by the weakened N···H−O bond, as the N···H distance in **4** (1.903 Å) became significantly longer than the N···H distance in **3** (1.815 Å) (see Scheme 1). Therefore, the rotational barrier of **4** could still be a close estimation for that of **1**.

Effect of Temperature on Hydrogen Bonding. In order to obtain additional information about the rotamer conversion, **7** was further examined by ^{1}H NMR at variable temperature (Figure S8, Supporting Information). In deuterated 1,1,2,2-tetrachloroethane solvent, the compound is predominantly in the form of rotamer **7b**, on the basis of the chemical shift of phenolic proton H_a at 11.66 ppm (at 25 °C). As the temperature was increased, the signal of H_a gradually shifted upfield to 11.4 ppm at 140 °C (Figure S7, Supporting Information), while the phenyl protons were not shifted. Plot of temperature versus the chemical shift exhibited very good linear correlation for both **7** and **1** (Figure 6), showing that no dramatic chemical event occurred within the temperature range (−50 to 140 °C) examined. It appeared that the hydrogen bonding was strengened at the lower temperature, which led to gradual downfield shift of the phenolic proton signal. The similar temperature effect has been reported in the O−H···N hydrogen bond of 2-diethylaminomethyl-3,4,6-trichlorophenol.[24]

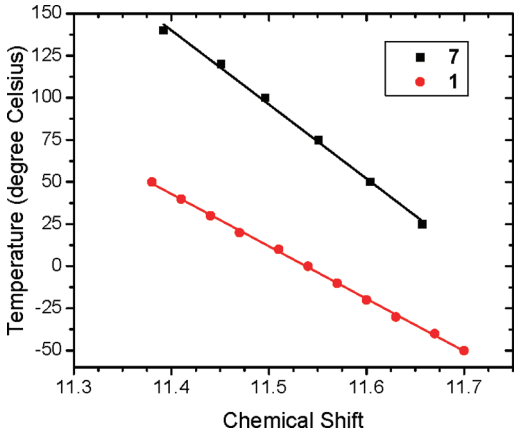

Figure 6. Temperature dependence of phenolic proton of **1** (in $CDCl_3$) and **7** (in $CDCl_2CDCl_2$).

CONCLUSION

We have designed a HBO derivative **4** as a model compound to determine the rotational barrier between different rotamers. By acquiring ^{1}H NMR spectra at variable temperature, the rotational barrier is calculated to be about 10.59 kcal/mol. From X-ray crystal structure and solution ^{1}H NMR of **3**, the chemical shift at ∼12 ppm is assigned to the rotamer with O−H···N hydrogen bonding (not O−H···O bonding). Identification of a specific rotamer is further confirmed by using model compound **7**, whose NOESY spectrum contains detectable signals from only one rotamer in the solution. Although the two HBO rotamers **1a** and **1b** are found in 1:1 ratio in the crystalline state, the chemical shift of phenolic proton and predominant *keto* emission in fluorescence suggests that **1b** is the major component in solutions of nonprotic solvent. On the basis of ^{1}H NMR analysis, only rotamer **1b** is detected in chloroform solution, which is very different from the rotamer ratio of 1:1 observed in the crystalline state. The study further reveals that the solvated structure could play a significant role in the *enol* emission.

EXPERIMENTAL SECTION

All reagents were purchased from commercial suppliers and used without further purification. Compound **1**, 2-(2′-hydroxyphenyl)benzoxazole (HBO), was synthesized following ref 25. Compound **4** was synthesized as described in our previous report.[15] Chromatographic purifications were carried out with silica gel of mesh 200−300. NMR spectra were collected on a 300 or 400 MHz spectrometers in $CDCl_3$ ($CDCl_3$: ^{1}H 7.27 ppm, ^{13}C 77.2 ppm). UV−vis spectra were acquired on a diode-array spectrometer. Emission spectra were obtained on a fluorescence spectrometer. Mass spectra were determined on time-of-flight (TOF) mass spectrometers equipped with MALDI ion sources.

Compound 3. 2,6-Dimethoxybenzaldehyde (300 mg, 1.8 mmol) and 2-aminophenol (197 mg, 1.8 mmol) were refluxed in toluene (20 mL) for 8 h. The reaction mixture was cooled to room temperature, and the precipitate was filtered to provide the Schiff base as a reddish powder: ^{1}H NMR ($CDCl_3$ 300 MHz) δ 9.14 (s, 1H), 7.32 (m, 2H), 7.14 (t, 1H, J = 8.1 Hz), 6.96 (d, 1H, J = 7.8 Hz), 6.86 (t, 1H, J = 7.8 Hz), 6.63 (d, 2H, J = 7.8 Hz), 3.90 (s, 6H). The Schiff base intermediate was transferred to a 25 mL round-bottomed flask equipped with a side arm, a magnetic stirring bar, and a connecting tube. Then $Pd(OAc)_2$ (2.3 mg, 0.01 mmol), Cs_2CO_3 (130 mg, 0.4 mmol), and 10 mL DMF were added. The mixture was stirred at room temperature for 5 min and then warmed to 80 °C, while the oxygen gas was

dx.doi.org/10.1021/jo201890f | J. Org. Chem. 2012, 77, 285−290

bubbled into the flask below the surface of the liquid. The progress of the reaction was monitored by ^{1}H NMR spectroscopy, which revealed the disappearance of the imine resonance at around δ 8.8 ppm when the reaction was complete. Upon completion of the reaction, the mixture was poured into 20 mL of water. The precipitate was collected by vacuum filtration and washed with 5 mL of water. The solid was redissolved in 20 mL of dichloromethane, washed with 1% EDTA aqueous solution (to remove the palladium catalyst), and then washed with water. The organic layer was dried over anhydrous Na_2SO_4. Removal of solvent afforded 2-(2,6-dimethoxyphenyl)benzoxazole-(DMHBO) as white solid (391 mg, 85% from 2,6-dimethoxybenzaldehyde): ^{1}H NMR ($CDCl_3$, 300 MHz) δ = 11.59 (s, 1H), 8.13 (d, 1H, J=2.4 Hz), 7.51 (m, 3H), 7.32 (m, 4H), 7.02 (d, 1H, J = 8.7 Hz), 2.63 (s, 3H); ^{13}C NMR ($CDCl_3$, 75 MHz) δ = 161.2, 157.6, 149.5, 137.7, 136.6, 136.0, 129.3, 126.6, 119.6, 119.4, 118.9, 112.5, 111.4, 111.1, 22.0. Boron tribromide (0.1 mL of 1 M BBr_3 in hexanes, 0.1 mmol) was added to a stirring mixture of DMHBO (50 mg, 0.2 mmol) in anhydrous CH_2Cl_2 (5 mL), and the reaction was stirred at room temperature under a nitrogen atmosphere. After 48 h, the reaction was quenched with MeOH (1 mL), and the reaction mixture was extracted with EtOAc (10 mL) and washed with H_2O (2 × 5 mL) and brine (5 mL). The organics were then filtered, dried over Na_2SO_4, and concentrated on a rotatory evaporator. Purification over a silica column with (4:1 hexane/EtOAc) afforded compound **3** as a white solid (39 mg, 82%). The obtained pure product was recrystallized from hexane/CH_2Cl_2 (2:1) to give white needle-like crystals (mp 180−181 °C): ^{1}H NMR ($CDCl_3$ 300 MHz) δ 12.90 (s, 1H), 7.68 (m, 2H), 7.27 (m, 3H), 6.77 (d, 1H, *J* = 9 Hz), 6.53 (d, 1H, *J* = 9 Hz, 1H), 4.01 (s, 3H); ^{13}C NMR ($CDCl_3$, 75 MHz) δ 163.2, 161.1, 159.4, 138.6, 133.5, 125.1, 124.9, 118.7, 111.0, 110.3, 102.1, 101.1, 56.3; HRMS (*m*/*z*) $[M + H]^+$ calcd for $C_{14}H_{11}NO_3$ 242.0817, found, 242.0816; IR (KBr) ν_{max}(cm^{-1}) 3034 (w), 2898 (w), 1638 (m), 1594 (m), 1543 (s), 1505 (s), 1284 (s), 1226 (s), 1055 (m), 998 (m), 821 (s).

Compound 7. 2-amino-3-methylphenol (25 mg,0.2 mmol) and 5-bromo-2-hydroxybenzaldehyde(40 mg, 0.2 mmol) were refluxed in absolute ethanol (15 mL) for 5 h. The reaction mixture was cooled to room temperature, and the precipitated Schiff base was filtered and transferred to a 25 mL round-bottomed flask equipped with a side arm, a magnetic stirring bar, and a connecting tube. Then $Pd(OAc)_2$ (2.3 mg, 0.01 mmol), Cs_2CO_3 (130 mg, 0.4 mmol), and 10 mL of DMF were added. The mixture was stirred at room temperature for 5 min and then warmed to 80 °C, while oxygen gas was bubbled into the flask below the surface of the liquid. The progress of the reaction was monitored by ^{1}H NMR spectroscopy, which revealed the disappearance of the imine resonance at around δ 8.8 ppm when the reaction was complete. Upon completion of the reaction, the mixture was poured into 20 mL of water. The precipitate was collected by vacuum filtration and washed with 5 mL of water. The solid was redissolved in 20 mL of dichloromethane, washed with 1% EDTA aqueous solution (to remove the palladium catalyst), and then washed with water. The organic layer was dried over anhydrous Na_2SO_4. Removal of solvent afforded the compound **7** (56 mg, 92%). Crystals suitable for X-ray analysis were obtained from dichloromethane: ^{1}H NMR ($CDCl_3$, 300 MHz) δ 11.59 (s, 1H), 8.13 (d, 1H, J=2.4 Hz), 7.51 (m, 3H), 7.32 (m, 4H), 7.02 (d, 1H, J = 8.7 Hz), 2.63 (s, 3H); ^{13}C NMR ($CDCl_3$, 75 MHz) δ 161.2, 157.6, 149.5, 137.7, 136.6, 136.0, 129.3, 126.6, 119.6, 119.4, 118.9, 112.5, 111.4, 111.1, 22.0; HRMS (*m*/*z*) $[M + H]^+$ calcd for $C_{14}H_{11}BrNO_2$ 303.9973, found 303.9978; IR (KBr) ν_{max} (cm^{-1}) 3065 (w), 2925 (m), 1627 (m), 1584 (m), 1541 (s), 1483 (s), 1453 (s), 1278 (s), 1251 (s), 831 (m), 777 (s).

■ ASSOCIATED CONTENT

Supporting Information

Crystal structures of **3** and **4**, ^{1}H NMR spectrum of **3**, and ^{1}H NMR of **1**, **4**, and **7** at variable temperatures. This material is available free of charge via the Internet at http://pubs.acs.org.

■ AUTHOR INFORMATION

Corresponding Author

*E-mail: yp5@uakron.edu.

■ ACKNOWLEDGMENTS

This work was supported by The University of Akron and Coleman Endowment. We also thank the National Science Foundation (CHE-9977144) for funds used to purchase the NMR instrument used in this work and for partial support (DMR-0905120) to E.T. and L.L. We thank two reviewers for very helpful suggestions.

■ REFERENCES

(1) Williams, D. L.; Heller, A. *J. Phys. Chem.* **1970**, *74* (26), 4473−4480.
(2) Taki, M.; Wolford, J. L.; O'Halloran, T. V. *J. Am. Chem. Soc.* **2004**, *126* (3), 712−713.
(3) Ohshima, A.; Momotake, A.; Arai, T. *Tetrahedron Lett.* **2004**, *45*, 9377−9381.
(4) Xu, Y.; Pang, Y. *Chem. Commun.* **2010**, *46*, 4070−4072.
(5) Xu, Y.; Pang, Y. *Dalton Trans.* **2011**, *40* (7), 1503−1509.
(6) Chu, Q.; Medvetz, D. A.; Pang, Y. *Chem. Mater.* **2007**, *19* (26), 6421−6429.
(7) Vazquez, S. R.; Rodriguez, M. C. R.; Mosquera, M.; Rodriguez-Prieto, F. *J. Phys. Chem. A* **2007**, *111* (10), 1814−1826.
(8) Zhang, G.; Wang, H.; Yu, Y.; Xiong, F.; Tang, G.; Chen, W. *Appl. Phys. B: Lasers Opt.* **2003**, *76*, 677−681.
(9) Woolfe, G. J.; Melzig, M.; Schneider, S.; Doerr, F. *Chem. Phys.* **1983**, *72* (2), 213−221.
(10) Das, K.; Sarkar, N.; Majumdar, D.; Bhattacharyya, K. *Chem. Phys. Lett.* **1992**, *198* (5), 443−448.
(11) Tong, Y. P. *Acta Crystallogr. Sect. E* **2005**, *61* (9), o3076−o3078.
(12) Wu, J.; Liu, W.; Ge, J.; Zhang, H.; Wang, P. *Chem. Soc. Rev.* **2011**, *40*, 3483−3495.
(13) Das, K.; Sarkar, N.; Ghosh, A. K.; Majumdar, D.; Nath, D. N.; Bhattacharyya, K. *J. Phys. Chem.* **1994**, *98*, 9126−9132.
(14) Nagaoka, S.; Itoh, A.; Mukai, K. *J. Phys. Chem.* **1993**, *97*, 11385−11392.
(15) Chen, W.-H.; Pang, Y. *Tetrahedron Lett.* **2010**, *51* (14), 1914−1918.
(16) Chen, W.; Xing, Y.; Pang, Y. A *Org. Lett.* **2011**, *13* (6), 1262−1265.
(17) ^{1}H NMR chemical shift for protons on oxygen and nitrogen can be found, for example, in the following reference: Lambert, J. B.; Shurvell, H. F.; Lightner, D. A.; Cooks, R. G., *Organic Structural Spectroscopy*; Prentice: Upper Saddle River, NJ, 1998; pp 46−47.
(18) Bovey, F. A. In *Nuclear Magnetic Resonance Spectroscopy*; Academic Press: New York, 1988; pp 255−324.
(19) Reich, H. J. *J. Chem. Educ. Software* **3D2**, **1996**
(20) Takeda, N.; Miyata, O.; Naito, T. *Eur. J. Org. Chem.* **2007**, No. 9, 1491−1509.
(21) Hsieh, C. C.; Cheng, Y. M.; Hsu, C. J.; Chen, K. Y.; Chou, P. T. *J. Phys. Chem. A* **2008**, *112* (36), 8323−8332.
(22) Chen, W.; Pang, Y. *Tetrahedron Lett.* **2009**, *50*, 6680−6683.
(23) In practice, the cross-peak is unobservable when the proton−proton distance exceeds about 5 Å. Lambert, J. B.; Shurvell, H. F.; Lightner, D. A.; Cooks, R. G., *Organic Structural Spectroscopy*; Prentice Hall: NJ, 1998; pp135−138.
(24) Sobczyk, L. *Appl. Magn. Reson.* **2000**, *18*, 47−61.
(25) Ohshima, A.; Momotake, A.; Nagahata, R.; Arai, T. *J. Phys. Chem. A* **2005**, *109* (43), 9731−9736.